Cell

Cotranslocational Degradation Protects the Stressed Endoplasmic Reticulum from Protein Overload

Seiichi Oyadomari,[1] Chi Yun,[1] Edward A. Fisher,[2,3] Nicola Kreglinger,[2,3] Gert Kreibich,[3] Miho Oyadomari,[1] Heather P. Harding,[1,4] Alan G. Goodman,[5] Hanna Harant,[6] Jennifer L. Garrison,[7] Jack Taunton,[7] Michael G. Katze,[5] and David Ron[1,2,3,*]

[1] Skirball Institute of Biomolecular Medicine, New York University School of Medicine, New York, NY 10016 USA
[2] Department of Medicine, New York University School of Medicine, New York, NY 10016 USA
[3] Department of Cell Biology, New York University School of Medicine, New York, NY 10016 USA
[4] Department of Pharmacology, New York University School of Medicine, New York, NY 10016 USA
[5] Department of Microbiology, School of Medicine, University of Washington, Seattle, WA 98195 USA
[6] Novartis Institutes for BioMedical Research, A-1235 Vienna, Austria
[7] Department of Cellular and Molecular Pharmacology, University of California, San Francisco, San Francisco, CA 94107 USA
*Contact: ron@saturn.med.nyu.edu
DOI 10.1016/j.cell.2006.06.051

SUMMARY

The ER's capacity to process proteins is limited, and stress caused by accumulation of unfolded and misfolded proteins (ER stress) contributes to human disease. ER stress elicits the unfolded protein response (UPR), whose components attenuate protein synthesis, increase folding capacity, and enhance misfolded protein degradation. Here, we report that *P58^{IPK}/DNAJC3*, a UPR-responsive gene previously implicated in translational control, encodes a cytosolic cochaperone that associates with the ER protein translocation channel Sec61. P58^{IPK} recruits HSP70 chaperones to the cytosolic face of Sec61 and can be cross-linked to proteins entering the ER that are delayed at the translocon. Proteasome-mediated cytosolic degradation of translocating proteins delayed at Sec61 is cochaperone dependent. In *P58$^{IPK-/-}$* mice, cells with a high secretory burden are markedly compromised in their ability to cope with ER stress. Thus, P58^{IPK} is a key mediator of cotranslocational ER protein degradation, and this process likely contributes to ER homeostasis in stressed cells.

INTRODUCTION

Early steps in the biogenesis of secreted and transmembrane proteins take place in association with the endoplasmic reticulum (ER). Newly synthesized polypeptides or segments thereof are translocated into the ER lumen, where chaperones and protein-modifying enzymes promote their conversion into functional proteins that exit the organelle (Sitia and Braakman, 2003; Anken et al., 2005). The ER's capacity to process proteins is relatively limited, and the stress caused by accumulation of unfolded and misfolded proteins (ER stress) contributes to a number of important human diseases (Kaufman, 2002).

Cells respond to ER stress by activating an unfolded protein response (UPR), which limits new protein synthesis and promotes the expression of genes that enhance the organelle's capacity to process unfolded proteins (Patil and Walter, 2001). Degradation of misfolded proteins represents a third mechanism by which cells limit the burden of unfolded proteins in their ER and assumes great importance when ER function is compromised. A dedicated machinery targets misfolded proteins to a retrotranslocation channel for subsequent proteasomal degradation in the cytosol. Early work suggested that the anterograde translocation of nascent proteins and retrograde translocation of completed misfolded ones were mediated by the same channel; however, it is presently believed that these two processes are separated in time and place and that the degradation of misfolded ER proteins is largely a posttranslocational event (Tsai et al., 2002; Meusser et al., 2005).

ApoB100 is a notable exception to this rule. This large secreted protein normally assembles with lipids in the lumen of the ER of liver cells to form a lipoprotein particle (Fisher and Ginsberg, 2002; Hussain et al., 2003). Lipidation is required for folding of apoB100. A block in lipidation leads to cotranslocational degradation of apoB100, as the protein remains associated with the Sec61 channel (Mitchell et al., 1998; Pariyarath et al., 2001). Furthermore, whereas the extraction of conventional misfolded lumenal proteins from the ER is mediated by the multifunctional ATPase p97/Cdc48 (Ye et al., 2001), the degradation of

apoB100 requires cytosolic chaperones of the HSP70 and HSP90 class (Fisher et al., 1997; Gusarova et al., 2001). The dependence of apoB100 degradation on cytosolic chaperones and the association of this process with the Sec61 channel present intriguing similarities to the process by which binding of lumenal HSP70 promotes the translocation of proteins into the ER (Matlack et al., 1999). The latter process requires a translocon-associated DnaJ domain containing cochaperone to stimulate ATP hydrolysis and peptide binding by the lumenal HSP70 (Misselwitz et al., 1998); however, no such factor has been found for cotranslocational degradation of apoB100.

P58^{IPK} was first discovered as an inhibitor of the virally induced eIF2α kinase PKR (Barber et al., 1994). The encoding gene *P58^{IPK}/DnaJC3* was subsequently found to be UPR inducible (Lee et al., 2003), and P58^{IPK} also binds and inhibits the ER stress-inducible eIF2α kinase PERK (Yan et al., 2002; Van Huizen et al., 2003). Given the latter's role in attenuating protein synthesis in ER-stressed cells (Harding et al., 1999), these findings implicated P58^{IPK} in recovery of protein synthesis following dissipation of ER stress. However, the phenotype of the P58^{IPK} knockout is not easy to reconcile with a role restricted to attenuating eIF2α phosphorylation (Ladiges et al., 2005).

P58^{IPK}/DNAJC3 contains a functional DnaJ domain that promotes ATP hydrolysis by HSP70 chaperones (Melville et al., 1999). The bulk of P58^{IPK} consists of nine tetratricopeptide (TPR) repeats by which it binds eIF2α kinase(s) (Lee et al., 1994) and the highly conserved C-terminal segments of cytosolic HSP70 and HSP90 proteins (Melville et al., 1999; Brychzy et al., 2003). The study below was designed to address the possibility that, in addition to its known role as an inhibitor of eIF2α kinases, P58^{IPK} might also collaborate with cytosolic chaperone networks that function in ER-stressed cells.

RESULTS

P58^{IPK}'s PERK-Independent Function

PERK's *C. elegans* homolog, *pek-1*, is required for the survival of worms lacking the IRE1 (*ire-1*) arm of the unfolded protein response (Shen et al., 2001). Given that P58^{IPK} inhibits PERK (Yan et al., 2002), we were surprised that, not only did attenuation of worm's P58^{IPK} homolog (*dnj-7*) by RNAi fail to rescue the phenotype of (partial) inactivation of *pek-1* in an *ire-1* mutant strain (Figures 1A5, 1A6, and 1A7), but also, on its own, *dnj-7*(RNAi) markedly reduced the fitness of *ire-1* mutant animals (Figure 1A8). To follow up on this hint of *pek-1* independent function(s) of DNJ-7/P58^{IPK}, we compared the effects of *dnj-7*(RNAi) in wild-type and *pek-1*-deleted worms. *dnj-7*(RNAi) increased basal activity of the ER stress-inducible *hsp-4::gfp* (BiP) reporter in both wild-type and *pek-1*-deleted worms. Furthermore, *dnj-7*(RNAi) enhanced *hsp-4::gfp* expression in worms exposed to the ER stress-promoting drug tunicamycin, regardless of their *pek-1* genotype (Figures 1B and 1C).

These observations indicate that DNJ-7/P58^{IPK}'s role in ER-stressed cells is not restricted to antagonizing PEK-1/PERK's kinase activity. Furthermore, growth retardation by *dnj-7*(RNAi) in the mutant *ire-1* background suggested that attenuated DNJ-7/P58^{IPK} expression affects HSP-4 expression indirectly, by increased burden of misfolded proteins rather than directly by enhancing UPR signaling. Subsequent experiments were designed to understand these PERK-independent functions of P58^{IPK}.

P58^{IPK} Is a Peripheral Membrane Protein of the Rough ER that Associates with SEC61 and HSP70 Chaperones

Recombinant P58^{IPK} expressed in COS1 cells colocalized with ER markers (Yan et al., 2002). We confirmed this colocalization by immunostaining the endogenous protein in mouse fibroblasts (Figure S1A in the Supplemental Data available with this article online) and extended this analysis by examining P58^{IPK}'s association with subcellular fractions in mouse liver, a rich source of the protein. The vast majority of P58^{IPK} from the postmitochondrial supernatant was recovered in the buoyant membrane fraction by equilibrium density centrifugation. This association was disrupted by carbonate extraction, which indicates that P58^{IPK} is a peripheral membrane protein (Figure 2A). Hepatocytes have well-differentiated smooth and rough ERs, which are easily separable. P58^{IPK} comigrated with the rough ER markers Sec61α and ribophorin I following equilibrium density gradient centrifugation (Figure 2B). Interestingly, P58^{IPK} was also membrane associated in *PERK$^{-/-}$* cells (Figure S1B), suggesting that membrane anchoring of P58^{IPK} entails interactions with a different rough ER transmembrane protein.

P58^{IPK} liberated from membranes by digitonin and other mild detergents remained associated with a relatively large heterogeneous complex that migrates through a velocity gradient as a broad peak (Figure 2C). Unfortunately, none of the available anti-P58^{IPK} antisera or antibodies recognize the protein in this intact native complex, precluding its immunopurification. However, following denaturation and complex disassembly, P58^{IPK} is readily recognizable both by the previously described monoclonal antibodies and by the polyclonal antiserum we raised to the bacterially expressed protein (data not shown).

To further characterize this membrane-associated P58^{IPK}-containing complex, we radiolabeled wild-type and *P58$^{IPK-/-}$* fibroblasts, solubilized the membranes in detergent, and added the lysine-reactive reversible crosslinker DSP to the lysate. After quenching the crosslinker, the complex was denatured in urea and SDS, which dissociates noncovalently bound partners and exposes P58^{IPK} to our antibody. The denaturants were diluted and the radiolabeled P58^{IPK} was immunoprecipitated along with covalently bound partners. The addition of crosslinker yielded a P58^{IPK}-dependent doublet of ~40 kDa, along with other weaker bands (Figure 3A, compare lanes 4 and 5 with lanes 11 and 12). This doublet comigrated with radiolabeled Sec61α, a central component of the

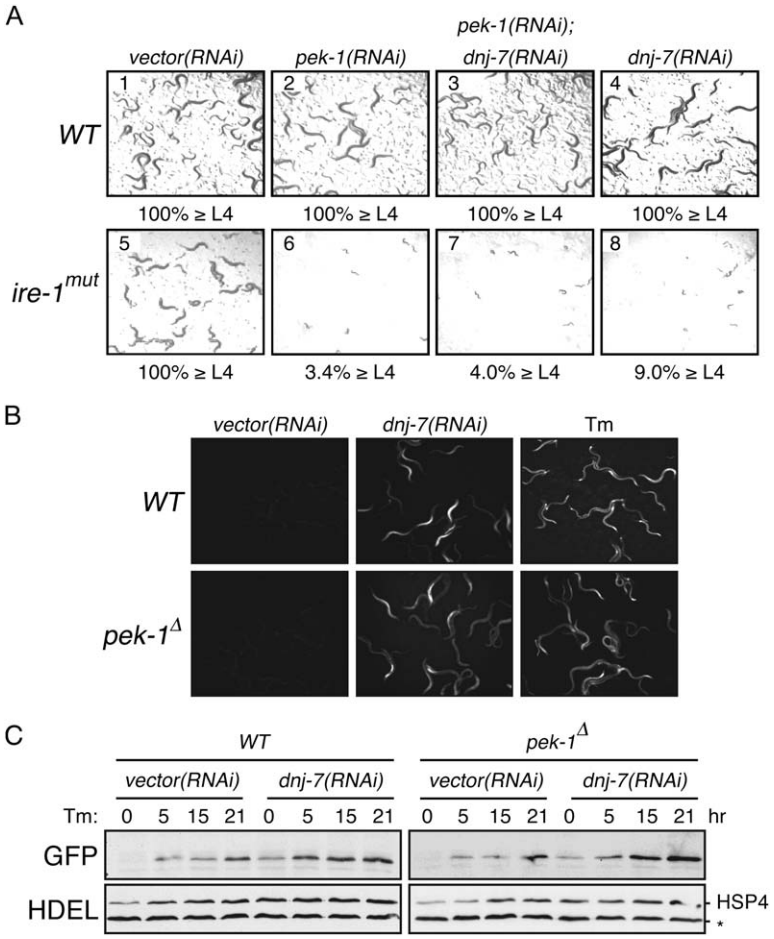

Figure 1. *PERK/pek-1*-Independent Activity of P58^{IPK}/*dnj-7*

(A) Photomicrographs obtained 72 hr after hatching of populations of wild-type (*WT*) and *ire-1* mutant (*ire-1^{mut}*) *C. elegans* that developed from fertilized eggs placed on bacterial lawns expressing the indicated RNAi gene constructs. The percentage of animals in the population that reached the L4 stage of development by 72 hr is indicated below the image.

(B) Fluorescent photomicrographs of the GFP signal of *hsp-4::gfp* transgenic animals of wild-type (*WT*) or *pek-1*-deleted (*pek-1$^{\Delta}$*) genotypes exposed to the indicated RNAi constructs or tunicamycin (30 μg/ml for 16 hr).

(C) Immunoblots of GFP protein and endogenous HSP-4/BiP (detected with anti-HDEL antibody) in lysates of untreated or tunicamycin-treated *hsp-4::gfp* transgenic animals of the indicated genotype and RNAi exposure. The asterisk marks an unidentified protein detected by the anti-HDEL antibody.

translocon (Figure 3A, lanes 17 and 18) and was reactive with anti-Sec61α antiserum, as revealed by the contents of an anti-Sec61α immunoprecipitation performed sequentially on the anti-P58^{IPK} immunoprecipitate after reversal of the crosslink (Figure 3A, lane 15). Furthermore, P58^{IPK} copurified with digitonin-solubilized native translocons, isolated by immunoprecipitation with a Sec61β antiserum in the absence of crosslinker (Figure 3B). These observations suggest that P58^{IPK} molecules are associated with the translocon.

The tetratricopeptide repeats (TPR) in P58^{IPK} closely resemble those found in TPR2, a protein of unknown function that binds avidly to HSP70 chaperones. P58^{IPK} has also been noted to form a complex with HSP70 in vitro (Melville et al., 1999), an observation that we confirmed (data not shown). TPR-containing proteins bind the conserved C-terminal tails of cytoplasmic HSP70 chaperones (Scheufler et al., 2000), and consistent with this observation, P58^{IPK} was co-eluted with HSP70 by excess ATP from an ATP-agarose affinity matrix loaded with detergent-solubilized ER membranes (Figure 3C). We also compared the colocalization of HSP70 chaperones with translocon components in velocity gradients prepared with digitonin-solubilized ER membranes from wild-type and *P58$^{IPK-/-}$* mouse liver. This mild solubilization procedure, which preserves the integrity of the translocon (Gorlich et al., 1992), yielded abundant comigrating HSP70 in the wild-type but not in the *P58$^{IPK-/-}$* sample (Figure 3D) and suggests that P58^{IPK} plays an important role in recruiting chaperones to the cytosolic face of the ER translocon.

P58^{IPK} and Cotranslocational Degradation of ER Proteins

The retrotranslocation of misfolded/misassembled proteins from the ER and their degradation in the cytoplasm requires numerous proteins on the cytosolic face of the ER (Tsai et al., 2002; Meusser et al., 2005); it is also a process whose disruption is predicted to promote accumulation of misfolded proteins in the ER lumen. Therefore, we measured the effect of the *P58^{IPK}* genotype on degradation of ectopically expressed T cell receptor α chain (TCRα), a well-characterized indicator of the activity of the ER retrotranslocation/degradation apparatus (Yu et al., 1997). In pulse-chase labeling experiments, newly synthesized TCRα decayed with similar kinetics in transfected wild-type and *P58$^{IPK-/-}$* cells (Figures 4A and 4B). While the *P58^{IPK}* genotype did not affect the decay of mature TCRα after the pulse, the amount of labeled

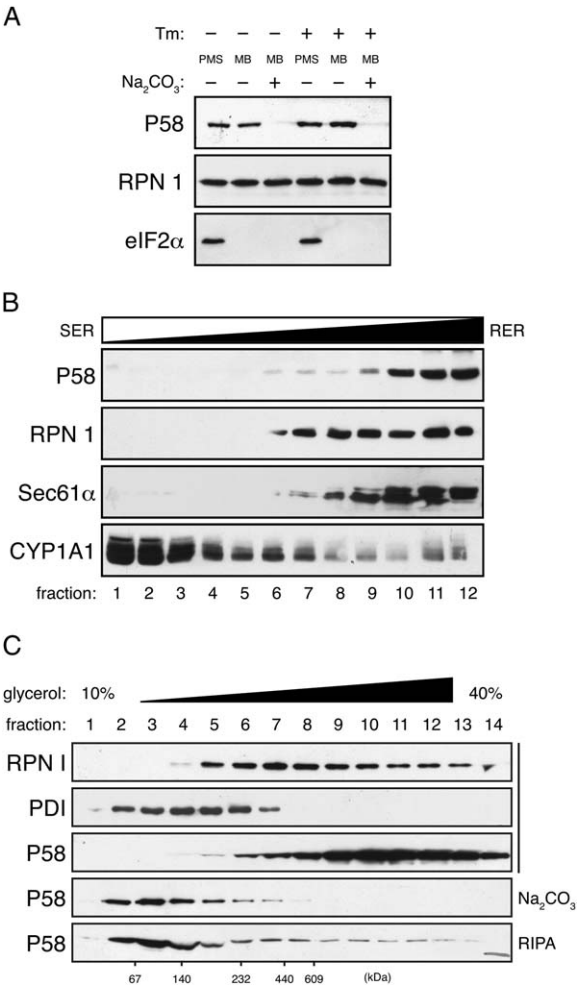

Figure 2. P58^{IPK} Is a Peripheral Membrane Protein of the Rough ER

(A) Immunoblots of P58^{IPK}, ribophorin I (RPN 1, an integral ER membrane marker), and eIF2α (a cytosolic marker) in postmitochondrial supernatant (PMS) or membrane fraction (MB) of liver from untreated and tunicamycin-treated mice; where indicated, the floated membranes were extracted with Na_2CO_3.

(B) Immunoblot of P58^{IPK}, ribophorin I (RPN I), and Sec61α (a rough ER [RER] marker) and Cyp1A1 (a smooth ER [SER] marker) content of fractions of a self-generated OptiPrep equilibrium gradient loaded with membranes procured by floatation from tunicamycin-treated mouse liver.

(C) Immunoblots of ribophorin I (RPN I), protein disulfide isomerase (PDI, a lumenal ER marker), and P58^{IPK} in fractions of a glycerol (velocity) gradient of digitonin-solubilized membranes of tunicamycin-treated mouse liver. Where indicated, the solubilized membranes were further exposed to RIPA or Na_2CO_3 before loading on the gradient. The migration of globular proteins of known size through the gradient is indicated.

TCRα present at the end of the (short) pulse was reproducibly higher in the *P58$^{IPK-/-}$* cells. This is unlikely to reflect differences in transfection efficiency or global protein synthesis, as accumulation of radiolabeled neomycin phosphotransferase (NPT, encoded by a separate gene on the TCRα plasmid) was similar in the two genotypes. Furthermore, the inhibitory effect of P58^{IPK} on the accumulation of ^{35}S-labeled nascent TCRα following a brief labeling pulse was recapitulated in transfected COS1 cells (Figure S2). Together, these experiments suggested that P58^{IPK} is dispensable for the posttranslocational degradation of mature TCRα but affects early step(s) in the biogenesis of ER proteins, prompting us to further explore the latter aspect.

Interfering with lipidation by blocking the microsomal triglyceride transfer protein (MTP) disrupts apoB100 translocation into the ER and renders it a substrate for an unconventional degradation process that initiates at the translocon and results in the delivery of the nascent chain to the cytoplasm for proteasomal degradation (Fisher and Ginsberg, 2002). Given evidence that P58^{IPK} functions in early steps of ER protein biogenesis, we chose to explore its effects on apoB100 degradation. Primary hepatocytes from wild-type and *P58$^{IPK-/-}$* mice were pulse-chase labeled in the presence or absence of an MTP inhibitor. The MTP inhibitor markedly reduced the level of full-length apoB100 that accumulated at the end of the pulse and destabilized the protein. This destabilization was prevented by treating cells with a proteasome inhibitor, as reported previously (Fisher et al., 1997). These effects of the MTP inhibitor were attenuated in the *P58$^{IPK-/-}$* cell, as reflected in the accumulation of more full-length apoB100 at the end of the pulse and marked stabilization of the protein during the chase (Figures 4C and 4D). ApoB48, an alternative product of the same gene whose biosynthesis is less dependent on lipidation, was less affected by the *P58^{IPK}* mutation, and the *P58^{IPK}* genotype had no effect on total protein synthesis in the presence or absence of the MTP inhibitor (data not shown). Furthermore, MTP inhibition increased the amount of newly synthesized apoB recovered by sequential co-immunoprecipitation in a crosslinked complex with P58^{IPK} (Figure 4E). Together, these observations suggest a direct role for P58^{IPK} in the degradation of apoB100 molecules whose translocation is compromised by defective lipid transfer.

ApoB100 is a special, ligand-dependent secreted protein; however, the observation that the amount of TCRα accumulating at the end of a short labeling pulse was also negatively affected by the expression of P58^{IPK} (Figure 4A and Figure S2) suggested that the cochaperone may contribute to the degradation of conventional ER proteins early during their biogenesis. However, detection of the nonglycosylated TCRα intermediate, predicted to serve as P58^{IPK}'s substrate in this degradation process, was unreliable (data not shown). Therefore, we sought a more robust system in which to test whether P58^{IPK}'s role in cotranslocational degradation is restricted to apoB100 or if the cochaperone contributes generally to the degradation of other ER proteins that translocate inefficiently.

Derivatives of a naturally occurring cyclodepsipeptide, HUN-7293, have been reported to selectively block the

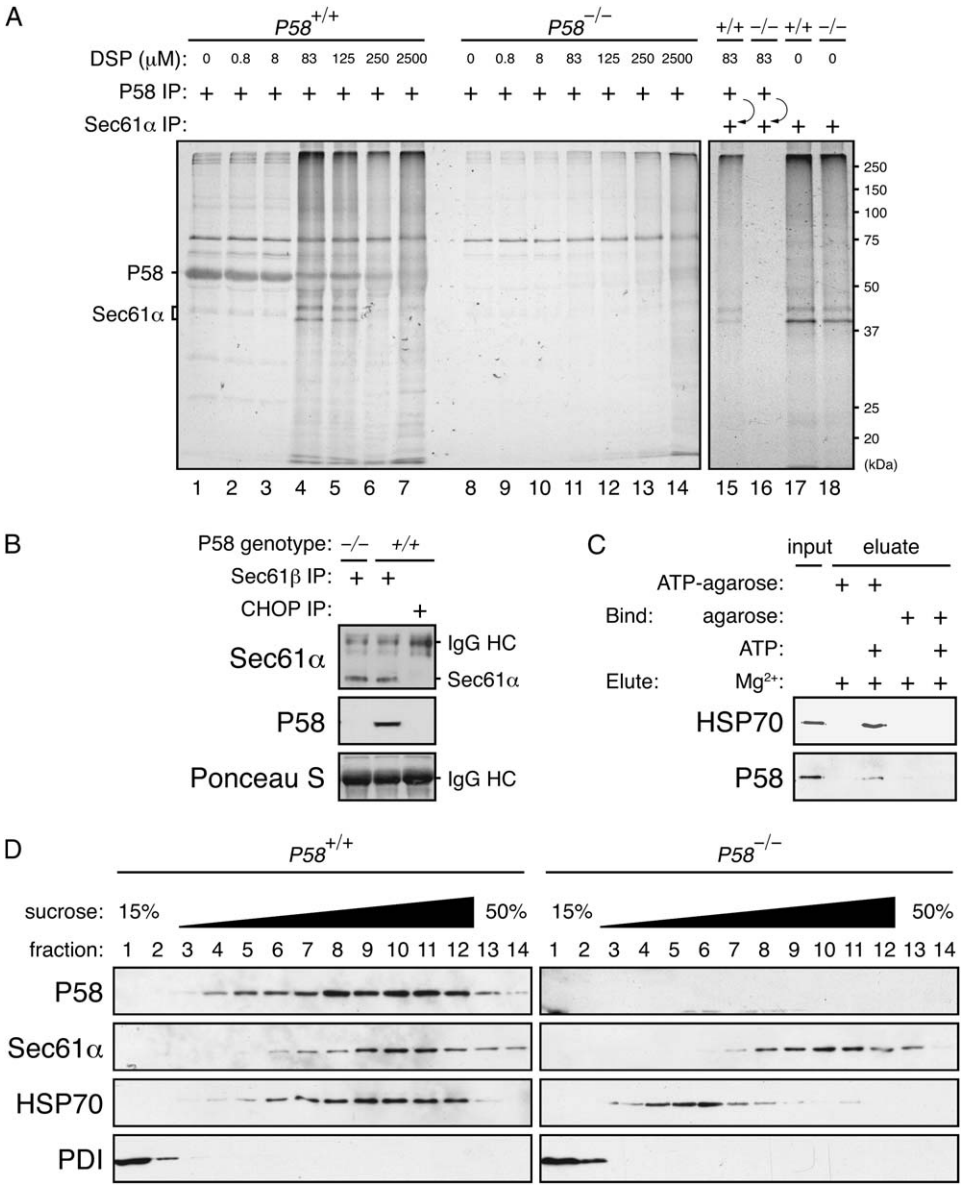

Figure 3. P58^{IPK} Is Associated with the ER Translocon and Cytosolic HSP70 Chaperones

(A) Autoradiograph of metabolically labeled P58^{IPK} and associated crosslinked proteins immunoprecipitated from wild-type (*P58*$^{+/+}$) and P58^{IPK} knockout (*P58*$^{-/-}$) mouse fibroblast lysate with the indicated antisera. The crosslink was reversed, and the individual radiolabeled proteins in half of the immunoprecipitated sample were resolved by SDS-PAGE (lanes 1–14). The other half was subsequently immunoprecipitated with antiserum to Sec61α (lanes 15 and 16) and loaded alongside an anti-Sec61α immunoprecipitate of uncrosslinked labeled lysate (lanes 17 and 18). The position of P58^{IPK} and Sec61α bands is indicated.

(B) Immunoblot of P58IPK and Sec61α in complexes recovered by an anti-Sec61β immunoprecipitate from digitonin-solubilized purified membrane fractions of liver from tunicamycin-treated wild-type (+/+) and P58IPK knockout (−/−) mice. Anti-CHOP antiserum was used to control for the specificity of the immunoprecipitation procedure, and the Ponceau S stain of the blot reveals the levels of immunoprecipitating IgG heavy chain (IgG HC) in the samples.

(C) Immunoblot of HSP70 and P58^{IPK} content of complexes purified by ATP-agarose affinity chromatography, or agarose affinity chromatography (as a specificity control) from detergent-solubilized membranes of tunicamycin-treated mouse liver. The complexes were eluted with $MgCl_2$ and ATP as indicated.

(D) Immunoblot of P58^{IPK}, Sec61α, HSP70, and protein disulfide isomerase (PDI) in fractions of a sucrose velocity gradient loaded with rough ER membranes purified from liver of tunicamycin-treated wild-type (*P58*$^{+/+}$) and P58^{IPK} knockout (*P58*$^{-/-}$) mice and solubilized with digitonin under conditions that preserve translocon integrity.

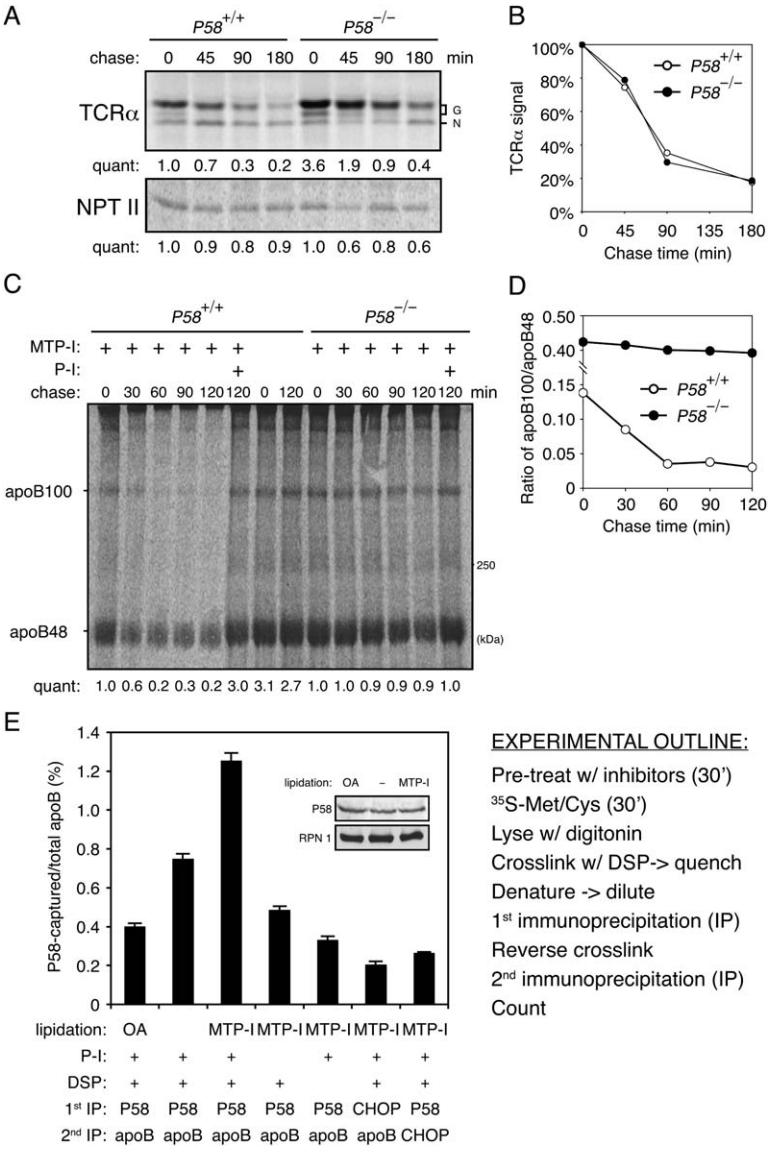

Figure 4. P58^{IPK} Is Required for Degradation of Nonlipidated apoB100 in Hepatocytes

(A) Autoradiograph of ^{35}S-labeled HA epitope-tagged T cell receptor α chain (TCRα) ectopically expressed in transfected wild-type (*P58*$^{+/+}$) and P58^{IPK} knockout (*P58*$^{-/-}$) mouse fibroblasts and immunoprecipitated from the cell lysate at the end of the 30 min metabolic labeling pulse or after the indicated period of cold chase. Radiolabeled neomycin phosphotransferase II (NPT II) expressed from the same plasmid serves as an internal control.

(B) Plot of the TCRα signal from (A).

(C) Autoradiograph of apoB immunoprecipitated from wild-type and *P58*$^{IPK-/-}$ cultured primary hepatocytes in a pulse-chase labeling experiment conducted in the presence or absence of a microsomal transfer protein inhibitor (MTP-I) or a proteasome inhibitor (P-I). The positions of apoB100 and apoB48 are indicated.

(D) Plot of the apoB100/apoB48 signal from (C).

(E) Quantification of radiolabeled apoB associated with P58^{IPK} following crosslinking with DSP and recovery by sequential immunoprecipitation (mean ± SEM), first with anti-P58^{IPK} serum and then (after reversal of the crosslink) by anti-apoB serum. Where indicated, the cells were exposed to oleic acid (OA, to promote lipidation) or MTP inhibitor (MTP-I, to block lipidation) and proteasome inhibitor (P-I) to block apoB degradation. The crosslinker (DSP) was omitted in sample 5, and the specific anti-P58^{IPK} and anti-apoB sera were replaced by the irrelevant anti-CHOP serum in samples 6 and 7. The amount of radiolabeled (apoB) protein recovered in the sequential immunopurification, measured by scintillation counting, is expressed as a fraction of the total radiolabeled apoB, recovered by direct immunoprecipitation from a parallel sample. The inset is an immunoblot of P58^{IPK} and ribophorin I, demonstrating that the experimental conditions used here did not affect protein levels in these cells.

translocation of human vascular cell adhesion molecule-1 (VCAM-1) into the ER. The stalled VCAM-1 (which lacks glycans and migrates faster than the mature form on SDS-PAGE) is rapidly degraded normally but accumulates at the translocon if proteasomes are inhibited (Besemer et al., 2005; Garrison et al., 2005). To determine if P58^{IPK} affects the fate of human VCAM-1 in cells treated with a translocation inhibitor, we compared the effects of an inhibitor, CAM741 (Besemer et al., 2005), on the fate of metabolically labeled human VCAM-1 expressed from a recombinant retrovirus in wild-type and *P58*$^{IPK-/-}$ mouse fibroblasts. Micromolar concentrations of CAM741 led to accumulation of a higher-mobility form of human VCAM-1 in the mutant but not in the wild-type cells (Figure 5A, lanes 5 and 6). A species of indistinguishable mobility accumulated in both wild-type and mutant CAM741-treated cells when exposed to a proteasome inhibitor (Figure 5A, lanes 7 and 14). The latter corresponds to the labile, nonglycosylated pre-VCAM-1 whose translocation is blocked by the inhibitor (Besemer et al., 2005; Garrison et al., 2005). A slightly faster-migrating species, presumed to reflect translocated but unglycosylated VCAM-1, whose signal peptide had been cleaved, was observed in cells treated with the glycosylation inhibitor tunicamycin (Figure 5A, lane 15; and Figure S3). Furthermore, at lower concentrations (50–200 nM) CAM741 was less effective in blocking the accumulation of mature, glycosylated VCAM-1 in cells lacking P58^{IPK} (Figure 5A, compare lanes 2–4 with 9–11).

COS1 cells express low levels of detectable endogenous P58^{IPK} (Figure 5B); therefore, we examined the effect of enforced expression of P58^{IPK} on the fate of VCAM-1 in

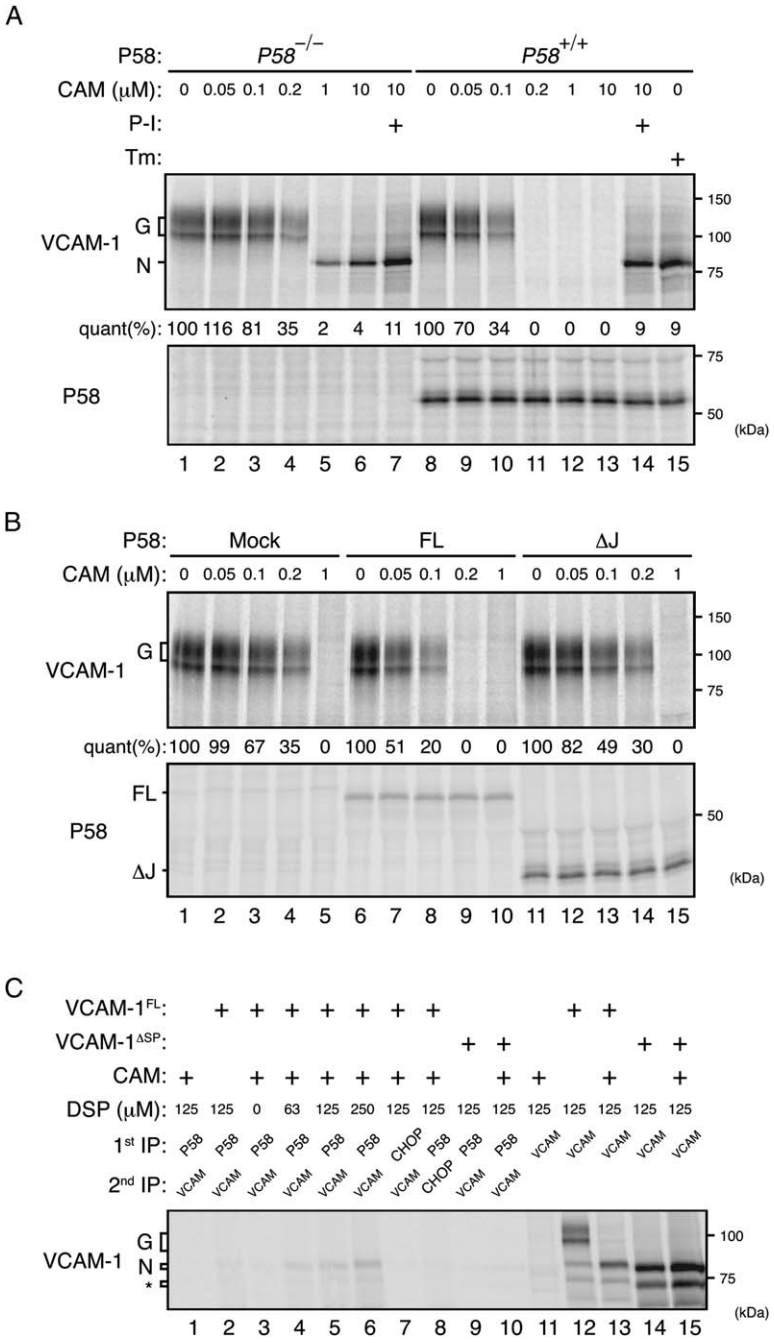

Figure 5. P58^{IPK} Promotes Cotranslocational Extraction of Human VCAM-1 in Cells Exposed to a Specific Translocation Inhibitor

(A) Autoradiogram of metabolically labeled human VCAM-1 expressed from a recombinant retrovirus in *P58$^{IPK+/+}$* and *P58$^{IPK-/-}$* mouse fibroblasts. The cells were exposed to the indicated concentration of CAM741 ("CAM"), tunicamycin (Tm), or proteasome inhibitor (P-I) for the duration of the 4 hr labeling pulse, followed by lysis and immunoprecipitation with a rabbit immune serum that recognizes both translocated (glycosylated ["G"]) and nontranslocated (nonglycosylated ["N"]) VCAM-1. The mature VCAM-1 signal was quantified in each lane and is expressed as a fraction of the signal in untreated cells.

(B) Autoradiogram of metabolically labeled human VCAM-1 expressed by transfection in COS1 cells or coexpressed together with wild-type P58^{IPK} (FL) or mutant P58^{IPK} lacking the effector J domain (ΔJ). The cells were treated with CAM741 as in (A). The lower panel is an autoradiograph of P58^{IPK} (full-length [FL] and mutant [ΔJ]), immunopurified from the flow-through of the VCAM-1 immunopurification.

(C) Autoradiogram of radiolabeled VCAM-1 associated with P58^{IPK} in cotransfected COS1 cells, following crosslinking with DSP and recovery by sequential immunoprecipitation, first with anti-P58^{IPK} serum and then (after reversal of the crosslink and denaturation of the sample) by anti-VCAM-1 serum. The cells were exposed to CAM741 (1 μM to inhibit VCAM-1 translocation) and proteasome inhibitor to block degradation of the stalled VCAM-1. CAM741 was omitted in lane 2, the crosslinker (DSP) was omitted in lane 3, the specific anti-P58^{IPK} and anti-VCAM sera were replaced with the irrelevant anti-CHOP serum in lanes 7 and 8, and a truncated form of VCAM-1 lacking the signal peptide (VCAM-1$^{\Delta SP}$) was used in lanes 9 and 10. Lanes 11–15 are of VCAM-1 immunopurified from the flow-through of lanes 1–3 and 9–10, as indicated. The asterisk marks an unidentified protein that is variably immunopurified with the VCAM-1 antisera and may represent a degradation product.

these cells (characterization of VCAM-1 proteins in COS1 cells is presented in Figure S3). Wild-type, but not mutant P58^{IPK}ΔJ (lacking the effector J domain), sensitized COS1 cells to the inhibitory effects of CAM741 on mature human VCAM-1 expression (Figure 5B), indicating that P58^{IPK} can be limiting for the inhibitory effect of CAM741.

To further characterize the interaction between P58^{IPK} and VCAM-1, we determined the effect of CAM741 on the recovery of VCAM-1 in a crosslinked complex with P58^{IPK} by sequential immunoprecipitation from radiolabeled COS1 cells that had been treated with a proteasome inhibitor. A crosslinker-dependent and antisera-dependent radiolabeled band of similar mobility to nonglycosylated VCAM-1 was recovered in complex with P58^{IPK} in cells treated with CAM741 (Figure 5C). Neither mature VCAM-1 nor a truncated VCAM-1 lacking the signal peptide interacted with P58^{IPK}, arguing against postlysis associations. Together, these observations point to a direct role for P58^{IPK} in extraction of nascent human VCAM-1 from the translocon under conditions in which translocation is

partially inhibited and in delivery of the stalled protein to the downstream degradation machinery when translocation is completely inhibited.

An ER Stress Disease Model Uncovers a Requirement for P58^{IPK}

To determine if P58^{IPK}'s role in degrading proteins that are delayed at the translocon correlates with a physiologically significant impairment in coping with ER stress, we turned to the *P58^{IPK}* knockout mice. As an isolated mutation in a C57BL/6 background, *P58$^{IPK+/-}$* animals are normal and *P58$^{IPK-/-}$* mice have a very mild phenotype, manifesting as a mild delay in postnatal growth in both sexes and subclinical glucose intolerance developing in males by 6 months of age, which progresses to fasting hyperglycemia at 1 year of age in some animals (Ladiges et al., 2005; Figure 6).

The "Akita" mutation, C96Y in the A chain of the *Ins2* gene product, leads to pro-insulin misfolding and compromised ER function. The β cell adapts to this stress by activating the UPR, and on the C57BL/6 background *Ins2$^{+/C96Y}$* "Akita" animals are fairly well compensated; females are virtually asymptomatic and males develop progressive glucose intolerance culminating in a well-tolerated nonketotic chronic hyperglycemia (Oyadomari et al., 2002). Induction of P58^{IPK} is part of the adaptation of *Ins2$^{+/C96Y}$* "Akita" β cells to ER stress, as reflected in elevated P58^{IPK} staining in the affected endocrine pancreas (Figure 6A). Therefore, we chose to examine the importance of P58^{IPK} in this well-characterized ER stress-mediated disease model.

Compared to *Ins2$^{+/C96Y}$;P58$^{IPK+/-}$* mice (which are themselves indistinguishable from *Ins2$^{+/C96Y}$;P58$^{IPK+/+}$*), *Ins2$^{C96Y/+}$;P58$^{IPK-/-}$* mice were dramatically compromised: their growth as pups was severely retarded, and overt hyperglycemia set in within days after weaning in both sexes (Figure 6B). The elevated blood glucose was not met by a corresponding increase in plasma insulin; rather, plasma insulin levels were very low (Figure 6C), a finding that correlates with dramatic loss of islet mass (Figure 6D). These findings indicate that P58^{IPK} has an important role in preserving function of ER-stressed β cells.

The phenotype of the compound mutant mice is consistent with a role for P58^{IPK}-mediated cotranslocational degradation in promoting survival of ER-stressed β cells. However, the evanescence of the islets in the compound mutant mice precluded more detailed characterization of P58^{IPK}'s role in that system. Therefore, to explore the potential effect of ER stress on P58^{IPK} activity, we compared the physical interaction between P58^{IPK} and metabolically labeled nascent proteins in unstressed and ER-stressed cultured fibroblasts. Confining the analysis to nascent proteins favors detection of interactions between P58^{IPK} and its clients (over interactions with radiolabeled mature cofactors). To avoid the confounding effects of changing levels of P58^{IPK}, we induced ER stress with a brief pulse of thapsigargin (an agent that adversely affects the protein folding environment in cells within minutes of application) and we minimized the inhibitory effect of ER stress on protein synthesis by conducting the experiment in the presence of serum (Harding et al., 1999).

Cells were untreated or pretreated with thapsigargin for 30 min followed by a brief 10 min labeling pulse conducted in the presence of a low concentration of puromycin. The latter integrates randomly into radiolabeled nascent chains, releasing them from the ribosome with a covalent bound C-terminal puromycin moiety that is reactive with a specific antiserum (Zhang et al., 1997). Following solubilization with digitonin and crosslinking with DSP, the lysate was denatured in 2% SDS, disrupting noncovalent interactions. The SDS was diluted and P58^{IPK} (and associated radiolabeled proteins) was immunoprecipitated. The anti-P58^{IPK} immune complex was disrupted with 2% SDS, crosslinks reversed with DTT, and the radiolabeled, nascent, puromycinylated proteins were captured by a second immunoprecipitation reaction with an antisera to puromycin and quantified by scintillation counting. Interestingly, exposure to thapsigargin resulted in a 1.6-fold increase in the fraction of puromycinylated (nascent) proteins recovered in complex with endogenous P58^{IPK} (Figure 7A).

Several controls were included: the signal detected by sequential immunoprecipitation in cells radiolabeled in the absence of puromycin was negligible (Figure S4), and the experiment was conducted in *P58$^{IPK-/-}$* cells, in which thapsigargin did not increase recovery of puromycinylated proteins in the anti-P58^{IPK} immune complex. Exposure of wild-type cells to arsenite, an agent that mimics the effects of ER stress on the translational apparatus (reflected in eIF2α phosphorylation [see inset]) but causes little or no ER stress, very modestly increased complex formation (1.1-fold). Finally, combining, before crosslinking, lysates made from radiolabeled, thapsigargin, and puromycin-treated *P58$^{IPK-/-}$* cells and nonlabeled lysates from thapsigargin-treated wild-type cells yielded a low background signal, suggesting that the interactions immortalized by the crosslinking procedure do not reflect a postlysis artifact. While other interpretations cannot be excluded, the observation that most of the endogenous P58^{IPK} in cells is associated with RER membranes (Figure 2), suggests that the puromycinylated proteins associated with it are translocation substrates. This experiment is therefore consistent with an ER stress-mediated enhancement of P58^{IPK}'s interactions with its client proteins.

DISCUSSION

Previously characterized as a stoichiometric inhibitor of the stress-inducible eIF2α kinases PKR and PERK, P58^{IPK} emerges from these studies as having a broader role in the ER.

P58^{IPK} and Degradation of Stalled Translocation Substrates

Studies of several model proteins have shown that their degradation occurs after dissociation from the translocon

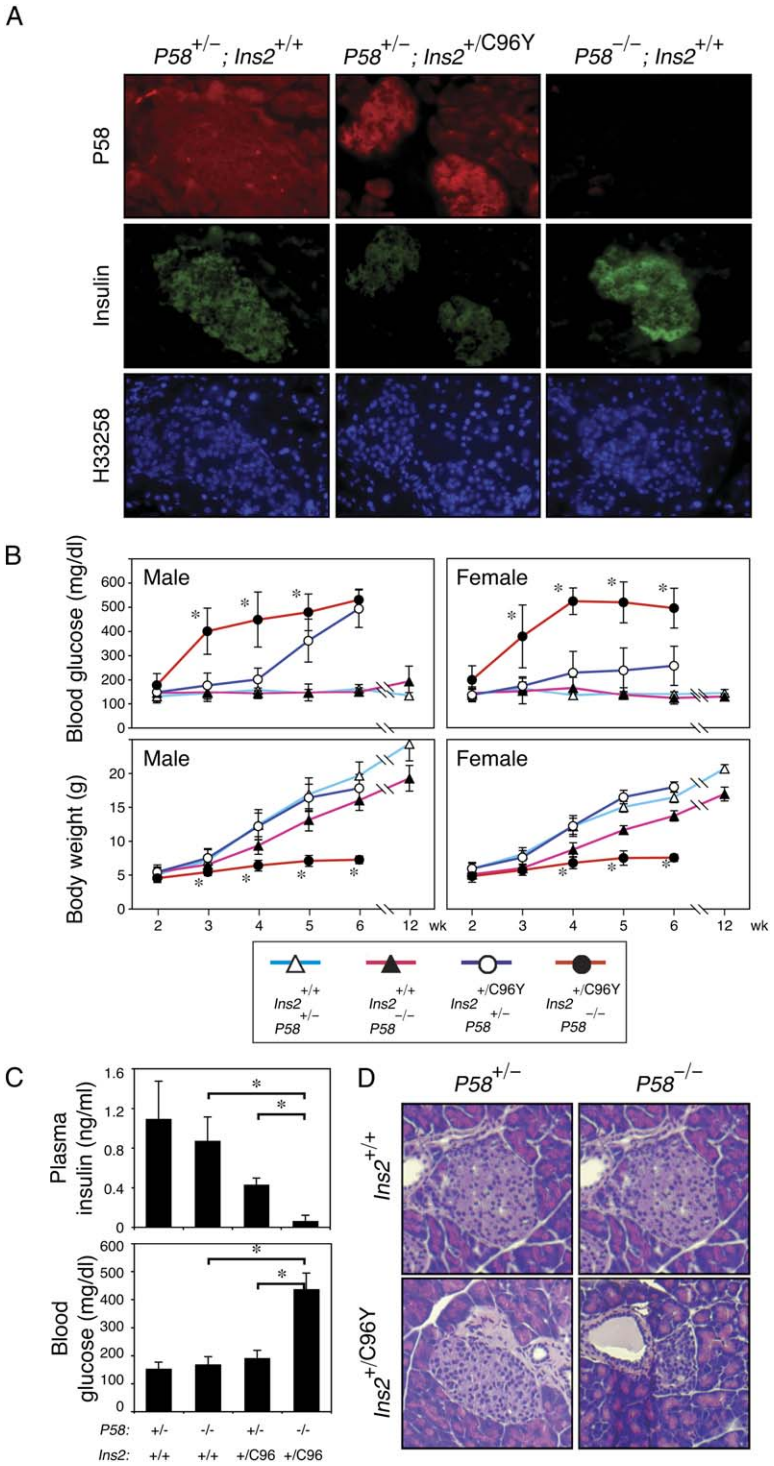

Figure 6. Loss of P58^{IPK} Sensitizes Mice to ER Stress-Induced Diabetes Mellitus

(A) Immunostaining of P58^{IPK} and insulin in sections of pancreas obtained from wild-type (*Ins2*$^{+/+}$) and "Akita" mutant mice (*Ins2*$^{+/C96Y}$). The H33258 signal reports on all the nuclei in the field.

(B) Time-dependent changes in blood glucose levels and body weight of male and female mice with the indicated *P58*^{IPK} and *Ins2* genotypes. Shown are means ± SD (n = 6; *p < 0.05 for *Ins2*^{C96Y};*P58*$^{+/-}$ versus *Ins2*^{C96Y};*P58*$^{-/-}$). Note that the compound mutant animals all died between 6 and 12 weeks.

(C) Plots of plasma insulin and blood glucose of 3-week-old female mice. Shown are means ± SD (n = 5; *p < 0.05).

(D) Photomicrographs of the pancreas of 3-week-old female mice with the indicated genotypes.

and release into the lumen (in the case of soluble proteins) or after lateral gating and partitioning into the lipid bilayer (in the case of integral membrane proteins). A retrotranslocation apparatus with components conserved in all eukaryotes identifies the misfolded protein and recruits it to a channel that is likely distinct from the translocon. Following channel engagement and with the assistance of cytosolic partners, the misfolded protein is retrotranslocated, polyubiquitinated, and delivered to the proteasome for degradation (Tsai et al., 2002; Meusser et al., 2005). We have no evidence that P58^{IPK} contributes to this process; rather, P58^{IPK} helps degrade proteins at the translocon, as

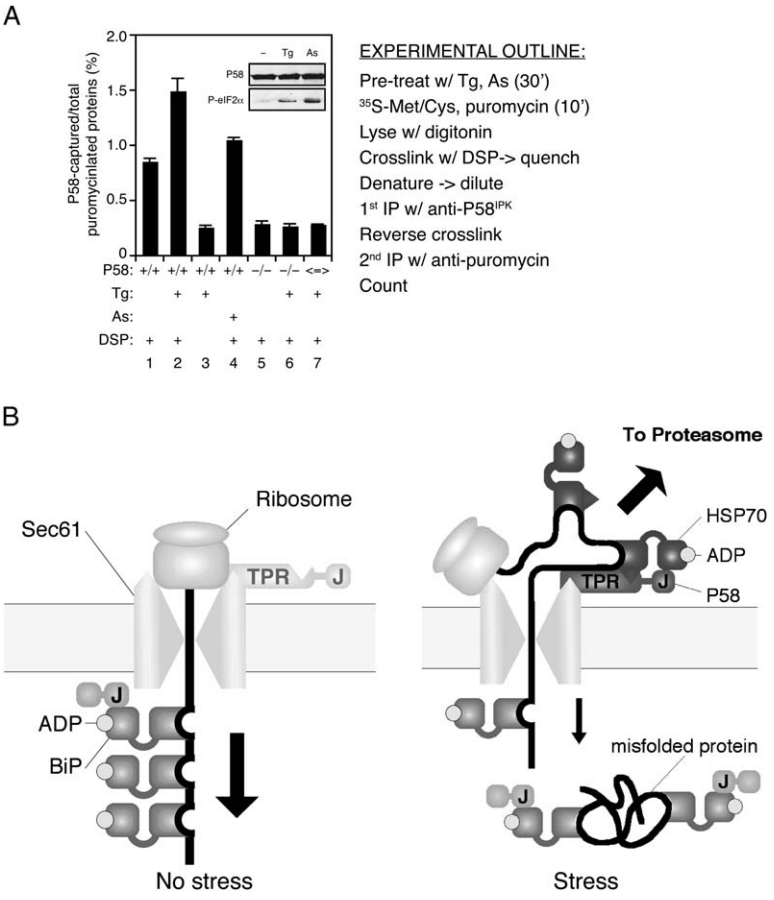

Figure 7. Increased Association of Endogenous P58^{IPK} with Nascent Polypeptides in ER-Stressed Cells

(A) Quantification of radiolabeled nascent (puromycinylated) proteins associated with endogenous P58^{IPK} following crosslinking with DSP and recovery by sequential immunoprecipitation, first with anti-P58^{IPK} serum and then (after reversal of the crosslink and dissociation of the immune complex) by anti-puromycin serum. Where indicated, mouse fibroblasts of wild-type and knockout *P58^{IPK}* genotype were treated with thapsigargin (Tg, 100 nM, to induce ER stress) or arsenite (25 μM, as a cytosolic stress control). The crosslinker (DSP) was omitted from sample 3, and radiolabeled extracts from –/– cells were combined with nonlabeled extracts from +/+ cells prior to crosslinking in sample 7 (labeled <=>). The amount of radiolabeled puromycinylated protein recovered in the sequential immunopurification was measured by scintillation counting and is expressed as a fraction of the total radiolabeled puromycinylated proteins, recovered by direct immunoprecipitation. Shown are the mean and range of an experiment performed in duplicate and repeated four times. The inset is that of a P58^{IPK} and P-eIF2α blot of lysates of cells exposed to thapsigargin or arsenite.

(B) Cartoon depicting P58^{IPK}'s hypothesized role at the translocon. In unstressed cells with ample reserves of lumenal chaperones (BiP and associated J domain cofactors), protein translocation proceeds efficiently. The ribosome-translocon junction is closed, and P58^{IPK} is inactive (left panel). In ER-stressed cells (right panel), accumulation of misfolded protein challenges lumenal chaperone reserves. The resulting inefficient protein translocation favors disruption of the ribosome-translocon seal and exposure of the cytosolic portion of the translocating polypeptide to P58^{IPK}. The latter recruits cytosolic HSP70s to the translocon and presents the client protein to them, thus promoting its extraction from the lumen through ATP hydrolysis, possibly by a ratcheting mechanism involving sequential binding of HSP70 molecules.

exemplified by its role in the degradation of apoB100 and VCAM-1.

ApoB100 degradation occurs while the protein remains associated with the translocon (Mitchell et al., 1998; Pariyarath et al., 2001); however, the process is incompletely understood. Especially obscure is the mechanism by which cytosolic proteins such as the chaperones known to assist in apoB100 degradation (Fisher et al., 1997; Gusarova et al., 2001) might gain access to the polypeptide. Engagement of the substrate at the translocon shields it from reactive probes applied to the cytosol side, findings that imply a tight ribosome-translocon junction (Crowley et al., 1994; Jungnickel and Rapoport, 1995). However, mounting evidence suggests that the seal on the ribosomal side might be modulated by events in the channel or possibly more distally in the lumen of the ER. For example, the signal sequence can influence the nascent chain's accessibility on the cytosolic side; when appended to a model translocated substrate, the efficient signal sequence from prolactin specifies a tight ribosome-translocon junction, whereas the weaker signal sequence of the prion-related protein specifies a weaker seal (Fons et al., 2003). Translocating apoB is likewise accessible to probes applied to the cytosolic side (Hegde and Lingappa, 1996).

While the relationship of accessibility on the cytosolic side to lipidation (and folding) on the lumenal side has not been explored directly, it is conceivable that misfolding associated with impaired lipidation retards translocation and disrupts the seal at the ribosome translocon junction. This, in turn, is predicted to expose the protein to P58^{IPK}, which is supported by the observation that inhibitors of lipidation increase the amount of radiolabeled apoB recovered in complex with P58^{IPK} (Figure 4E). We propose that P58^{IPK} uses its C-terminal DnaJ cochaperone domain to promote HSP70 chaperone binding to exposed regions of proteins whose translocation is delayed for any reason. Cycles of P58^{IPK}-coordinated cytosolic chaperone binding extract the misfolded substrate from the translocon by a ratcheting mechanism similar to that used by lumenal chaperones to promote anterograde translocation (Matlack et al., 1999).

The fate of VCAM-1 in cells exposed to low concentrations of the translocation inhibitor suggests that translocation and P58^{IPK}-mediated extraction (and degradation) are competing processes and that the partitioning of the substrate between these two fates is sensitive to the level of P58^{IPK} (and therefore modulated by the UPR). Accumulation of cytosolic VCAM-1 was only observed in knockout cells exposed to high concentrations of the inhibitor; at lower concentrations of inhibitor reduced expression of mature VCAM-1 was also observed in the mutant cells, but this was not associated with the accumulation of the nonglycosylated form (Figure 5A, lanes 3 and 4). These findings are consistent with the existence of (saturable) P58^{IPK}-independent mechanisms for degrading substrates that fail to translocate and would otherwise accumulate on the cytosolic face of the ER membrane.

Cotranslocational Degradation and ER Stress

Cotranslational translocation can proceed without lumenal chaperones, at least in vitro (Gorlich and Rapoport, 1993). However, their contribution to the efficiency of the process is suggested by observations that BiP and its translocon-associated J domain-containing cofactor, Sec63, are required in an in vitro reconstituted system that translocates proteins posttranslationally (Matlack et al., 1999) and in an in vitro system for cotranslational translocation (Brodsky et al., 1995). Furthermore, inactivation of BiP/Kar2p by a *ts* mutation leads to accumulation of translocation substrates in the yeast cytosol in vivo (Vogel et al., 1990). Based on these observations we propose that, under conditions of ER stress, translocation is compromised by limited lumenal chaperone reserve. As a consequence, diverse ER proteins, delayed at the translocon, become substrates for extraction and degradation mediated by P58^{IPK} and its cytosolic HSP70 partners. This speculation is supported by the observation that ER stress increases the association of nascent (puromycinylated) proteins with P58^{IPK} (Figure 7A). Therefore, we propose that the induction of P58^{IPK} in ER-stressed cells represents an attempt to shift the equilibrium in favor of extraction from the translocon and cytosolic degradation of proteins as outlined in cartoon form (Figure 7B).

P58^{IPK} knockout results in increased misfolded protein burden in the ER lumen and higher levels of ER stress signaling (Figure 1B and Figure S5). The markedly impaired survival of β cells of *P58$^{IPK-/-}$;Ins2$^{+/C96Y}$* "Akita" mice, compared with "Akita" mice with a functional *P58^{IPK}* allele, is consistent with the importance of cotranslocational degradation in protecting the stressed ER of secretory cells (though other roles for P58^{IPK} cannot be excluded). This protective effect might reflect a reduction in protein flux into the stressed ER's lumen. Alternatively, as the folding of complex proteins often entails interactions between distant segments on the linear polypeptide chain, stalled translocating proteins remain unfolded and engage chaperones on the lumenal side. The first line of defense against this threat is the PERK-mediated attenuation of translation initiation, which has no negative consequences on the processivity of translation or translocation and therefore on the rate of protein folding. Our studies suggest that P58^{IPK} induction represents a second line of defense, which by extracting stalled translocation substrates frees the bound lumenal chaperones to engage in other tasks and clears the translocon from obstructing difficult-to-fold polypeptides.

EXPERIMENTAL PROCEDURES

Cell Culture, Transfection, and Treatment

P58$^{IPK-/-}$ and *P58$^{IPK+/+}$* mouse embryo fibroblasts were prepared from embryonic day 13.5 progeny of heterozygous knockout mice (Ladiges et al., 2005). Radiolabeled HA-tagged TCRα, NHK-AT, and wild-type or ΔJ mutant (1-393) mouse P58^{IPK} was expressed by transient transfection using the FuGENE 6 lipid-mediated gene transfer (Roche) in fibroblasts and the DEAE-dextran method for COS1 cells and detected by immunoprecipitation as previously described (Yu et al., 1997). Mammalian expression plasmids for human VCAM-1 and its truncated derivative have been previously described (Besemer et al., 2005; Garrison et al., 2005).

Antisera, Immunoblotting, Immunoprecipitation, and Immunostaining

Antiserum to mouse P58^{IPK} (NY1165) was raised by injecting a rabbit with full-length mouse P58^{IPK} expressed in *E. coli* as a GST fusion protein and cleaved by thrombin. Its use in immunostaining is described is detail in Figure S1A. Insulin immunoreactivity was detected as previously described (Oyadomari et al., 2002).

Rabbit anti-mouse CYP1A1 was a gift of Virginia Black (NYU), antiserum to puromycin was a gift of Peter Walter (UCSF), and antiserum to human VCAM-1 and ribophorin I were raised in rabbit against the bacterially expressed protein. Other antisera were purchased from commercial sources and used according to the vendor's specifications: rabbit anti-human α-1-Antitrypsin (DAKO), rabbit anti-GFP (Molecular Probe), mouse anti-HSP70/HSC70 (Stressgen), rabbit anti-neomycin phosphotransferase II (NPT II; US Biological), mouse anti-PDI (Stressgen), rabbit anti-Sec61α (Affinity BioReagents), and anti-phospho-eIF2α (BioSource).

Subcellular Fractionation, Protein Purification, and Crosslinking

The liver of the untreated or tunicamycin-treated mice (i.p. injection, 1 mg/kg body weight, 16 hr) was mechanically disrupted by Teflon glass homogenizer in homogenization buffer (20 mM Tris-HCl [pH 7.5], 5 mM $MgCl_2$, 1 mM dithiothreitol, 250 mM sucrose, 10 μg/ml cycloheximide, 1 mM PMSF, 4 μg/ml aprotonin, and 2 μg/ml pepstatin A), and the postmitochondrial supernatant (PMS) was isolated by centrifugation. The PMS was adjusted to 30% OptiPrep (Axis-Shield), and total membranes were floated by centrifugation (250,000 × g, 3 hr) on 25% OptiPrep. After dilution of the OptiPrep and pelleting (100,000 × g, 1 hr), the membranes were resuspended in homogenization buffer containing 20% OptiPrep and subjected to equilibrium density centrifugation (350,000 × g, 2 hr) in a self-generated OptiPrep gradient to separate rough and smooth ER. Rough ER was recovered by pelleting the relevant membrane fraction, translocons were solubilized in 3% digitonin (Calbiochem), and the soluble material was subjected to non-equilibrium (velocity) gradient centrifugation in a 15%–50% sucrose gradient as described (Gorlich et al., 1992).

HSP70 proteins were purified from the digitonin-solubilized membrane preparation by ATP-agarose affinity chromatography and eluted in 5 mM $MgCl_2$ with or without 20 mM ATP.

Crosslinking of P58^{IPK} to translocon components was assayed in wild-type or *P58$^{IPK-/-}$* fibroblasts labeled for 16 hr with ^{35}S-Translabel, solubilized in 3% digitonin, and exposed to varying concentrations of dithio-bis-succinimidylpropionate (DSP, Pierce) on ice for 60 min. After

quenching the unreacted DSP with 100 mM Tris-HCl (pH 7.5), the sample was denatured by exposure to 6 M urea and 2% SDS at 37°C. Following 20× dilution of the denaturants, $P58^{IPK}$ was immunoprecipitated in RIPA buffer. The crosslink was reversed by incubating the sample in 100 mM dithiothreitol, 6 M urea, and 2% SDS at 37°C (we found that heating the sample led to substantial loss of Sec61α immunoreactivity). Half the sample was set aside for loading on an SDS-PAGE and the other half was diluted again and immunoprecipitated with antiserum to Sec61α, reduced, and denatured as described above and applied to the same SDS-PAGE. Under these conditions, Sec61α migrates as a doublet on SDS-PAGE (given the lack of S-S bonds or glycosylation sites, we attribute this heterogeneity to incomplete denaturation at the relatively low temperature required to retain solubility).

Detection of metabolically labeled apoB was adapted from the published procedure (Fisher et al., 1997) to accommodate the use of primary hepatocytes isolated from C57BL/6 adult male mice of wild-type and $P58^{IPK-/-}$ genotypes and cultured on type I collagen-coated plates in Waymouth's medium supplemented with 0.1 nM insulin. Cells were switched to DMEM with 10% of the normal methionine and cysteine content 30 min before addition of ^{35}S-TRANSlabel (MP Biomedicals) at 250 μCi/ml for 30 min, followed by cold chase. Cells were pretreated with 10 μM lactacystin (Boston Biochem) for 30 min and then treated with the MTP inhibitor (50 μM CP10447; Pfizer) and 10 μM lactacystin as indicated. Radiolabeled apoB was immunoprecipitated with antiserum raised to mouse apoB.

Radiolabeled apoB in complex with $P58^{IPK}$ was isolated from rat McA-RH7777 hepatoma cells by adapting a procedure to detect complexes of apoB and Sec61 (Pariyarath et al., 2001). The cells were metabolically labeled in the presence of proteasome inhibitor as above, treated with digitonin (Calbiochem), and exposed to DSP crosslinker. Quenching, complex disruption, and sequential immunoprecipitation were conducted as described above (for Sec61α). The total amount of apoB synthesized was recovered by immunoprecipitation from a parallel sample of cells + supernatant, and the fraction of apoB recovered in complex with $P58^{IPK}$ was determined as the ratio of the two measurements.

VCAM-1 biogenesis was followed by pulse-labeling and immunoprecipitation. Wild-type and $P58^{IPK-/-}$ mouse fibroblasts were infected with a recombinant retrovirus encoding human VCAM-1, whereas COS1 cells were transfected with a plasmid encoding VCAM-1, alongside plasmids encoding wild-type or ΔJ mutant mouse $P58^{IPK}$. Two days after gene transduction, the cells were exposed to varying concentrations of CAM741 (50 nM–10 μM) in the presence or absence of proteasome inhibitor or tunicamycin, as described (Besemer et al., 2005), radiolabeled for 4 hr, and immunoprecipitated with a rabbit polyclonal serum raised against the bacterially expressed protein that detects both native and nonnative human VCAM-1.

Complexes between human VCAM-1 and $P58^{IPK}$ were detected in cotransfected COS1 cells as described above. CAM741 (1 μM) and MG132 (10 μM) were added to the culture media 30 min before and throughout the 2 hr ^{35}S-TRANSlabel (ICN; 250 μCi/ml) labeling pulse. Complex solubilization, crosslinking, and sequential immunoprecipitation were performed as described above for the analysis of $P58^{IPK}$ and Sec61a complexes.

The methods used to purify and detect complexes between puromycinylated (nascent) proteins and $P58^{IPK}$ in mouse fibroblasts are described in detail in the Results section. Metabolic labeling was performed in methionine minus DMEM with 10% dialyzed fetal calf serum. Puromycin (Calbiochem; 0.3 μM) and ^{35}S-TRANSlabel (ICN; 250 μCi/ml) were added for 10 min before solubilization in digitonin and crosslinking.

C. elegans Genetics and Procedures

The *ire-1(zc14)II* mutant and *hsp-4::gfp(zcIs4)V* BiP-promoter GFP reporter fusion strains are available from the Caenorhabditis Genetics Center. The *pek-1* (PERK) deletion strain *pek-1(zcdf2)X* was bred into the *hsp-4::gfp(zcIs4)V* background using standard procedures. To study the effect of gene inactivation on larval development, gravid homozygous *ire-1(zc14)II* mutant animals were treated with bleach to release fertilized eggs, 100 of which were placed on a lawn *E. coli* transformed with the pPD129.36 plasmid expressing double-stranded RNA to *pek-1* or *dnj-7* ($P58^{IPK}$), or a mixture of both. The plates were photographed 72 hr later, and the fraction of progeny that reached the L4 stage was determined by counting individual animals.

Experimental Diabetes Mellitus in the Mouse

All experiments in mice were approved by the IACUC. "Akita" mice bearing the C96Y mutation in *Ins2* were purchased from Jackson Labs and were bred onto the $P58^{IPK}$ knockout background (Ladiges et al., 2005) to create $Ins2^{C96Y/+}$;$P58^{IPK-/+}$ animals. As $P58^{IPK+/-}$ mice are indistinguishable from the wild-type, $Ins2^{C96Y/+}$;$P58^{IPK-/+}$ animals were then crossed with $Ins2^{+/+}$;$P58^{IPK-/-}$ to yield compound animals with combinations of $Ins2^{+/+}$, $Ins2^{C96Y/+}$, $P58^{IPK+/-}$, and $P58^{IPK-/-}$ genotypes. Glycemic control was assessed weekly by measuring morning blood glucose. Plasma insulin levels were measured at sacrifice. Pancreata were fixed in 10% formaldehyde, paraffin embedded, sectioned in 5 μm, and stained with hematoxylin and eosin or immunostained for insulin and $P58^{IPK}$. Statistical analysis was performed by the unpaired two-tailed Student's t test.

Supplemental Data

The Supplemental Data include five figures and can be found with this article online at http://www.cell.com/cgi/content/full/126/4/727/DC1/.

ACKNOWLEDGMENTS

We thank Jennifer Hui, Kazutaka Araki, Rivka Jungreis, and Cristina Villagra (NYU) for their assistance with various phases of this project; Berndt Oberhauser and Shirley Wang (Novartis) for synthesis of CAM741 and construction of the VCAM1 plasmids; Ron Kopito (Stanford University) for the HA-tagged TCRa clone; Virginia Black (NYU) for the antiserum to CYP1A1; Peter Walter (UCSF) for the anti-puromycin antibody; and Ramanujan Hegde (NIH) and Cole Haynes (NYU) for advice. Supported by NIH grants DK47119 and ES08681 to D.R., HL58541 to E.A.F., and fellowships from JDRF and the Uehara Memorial Foundation to S.O. H.H. is employed by Novartis and owns stock options and restricted stock units. The authors have no other conflicting financial interests.

Received: November 14, 2005
Revised: May 1, 2006
Accepted: June 8, 2006
Published: August 24, 2006

REFERENCES

Anken, E., Braakman, I., and Craig, E. (2005). Versatility of the endoplasmic reticulum protein folding factory. Crit. Rev. Biochem. Mol. Biol. *40*, 191–228.

Barber, G.N., Thompson, S., Lee, T.G., Strom, T., Jagus, R., Darveau, A., and Katze, M.G. (1994). The 58-kilodalton inhibitor of the interferon-induced double-stranded RNA-activated protein kinase is a tetratricopeptide repeat protein with oncogenic properties. Proc. Natl. Acad. Sci. USA *91*, 4278–4282.

Besemer, J., Harant, H., Wang, S., Oberhauser, B., Marquardt, K., Foster, C.A., Schreiner, E.P., de Vries, J.E., Dascher-Nadel, C., and Lindley, I.J. (2005). Selective inhibition of cotranslational translocation of vascular cell adhesion molecule 1. Nature *436*, 290–293.

Brodsky, J.L., Goeckeler, J., and Schekman, R. (1995). BiP and Sec63p are required for both co- and posttranslational protein translocation into the yeast endoplasmic reticulum. Proc. Natl. Acad. Sci. USA *92*, 9643–9646.

Brychzy, A., Rein, T., Winklhofer, K.F., Hartl, F.U., Young, J.C., and Obermann, W.M. (2003). Cofactor Tpr2 combines two TPR domains and a J domain to regulate the Hsp70/Hsp90 chaperone system. EMBO J. *22*, 3613–3623.

Crowley, K.S., Liao, S., Worrell, V.E., Reinhart, G.D., and Johnson, A.E. (1994). Secretory proteins move through the endoplasmic reticulum membrane via an aqueous, gated pore. Cell *78*, 461–471.

Fisher, E.A., and Ginsberg, H.N. (2002). Complexity in the secretory pathway: The assembly and secretion of apolipoprotein B-containing lipoproteins. J. Biol. Chem. *277*, 17377–17380.

Fisher, E.A., Zhou, M., Mitchell, D.M., Wu, X., Omura, S., Wang, H., Goldberg, A.L., and Ginsberg, H.N. (1997). The degradation of apolipoprotein B100 is mediated by the ubiquitin-proteasome pathway and involves heat shock protein 70. J. Biol. Chem. *272*, 20427–20434.

Fons, R.D., Bogert, B.A., and Hegde, R.S. (2003). Substrate-specific function of the translocon-associated protein complex during translocation across the ER membrane. J. Cell Biol. *160*, 529–539.

Garrison, J.L., Kunkel, E.J., Hegde, R.S., and Taunton, J. (2005). A substrate-specific inhibitor of protein translocation into the endoplasmic reticulum. Nature *436*, 285–289.

Gorlich, D., and Rapoport, T.A. (1993). Protein translocation into proteoliposomes reconstituted from purified components of the endoplasmic reticulum membrane. Cell *75*, 615–630.

Gorlich, D., Prehn, S., Hartmann, E., Kalies, K.U., and Rapoport, T.A. (1992). A mammalian homolog of SEC61p and SECYp is associated with ribosomes and nascent polypeptides during translocation. Cell *71*, 489–503.

Gusarova, V., Caplan, A.J., Brodsky, J.L., and Fisher, E.A. (2001). Apoprotein B degradation is promoted by the molecular chaperones hsp90 and hsp70. J. Biol. Chem. *276*, 24891–24900.

Harding, H., Zhang, Y., and Ron, D. (1999). Translation and protein folding are coupled by an endoplasmic reticulum resident kinase. Nature *397*, 271–274.

Hegde, R.S., and Lingappa, V.R. (1996). Sequence-specific alteration of the ribosome-membrane junction exposes nascent secretory proteins to the cytosol. Cell *85*, 217–228.

Hussain, M.M., Shi, J., and Dreizen, P. (2003). Microsomal triglyceride transfer protein and its role in apoB-lipoprotein assembly. J. Lipid Res. *44*, 22–32.

Jungnickel, B., and Rapoport, T.A. (1995). A posttargeting signal sequence recognition event in the endoplasmic reticulum membrane. Cell *82*, 261–270.

Kaufman, R.J. (2002). Orchestrating the unfolded protein response in health and disease. J. Clin. Invest. *110*, 1389–1398.

Ladiges, W.C., Knoblaugh, S.E., Morton, J.F., Korth, M.J., Sopher, B.L., Baskin, C.R., MacAuley, A., Goodman, A.G., LeBoeuf, R.C., and Katze, M.G. (2005). Pancreatic beta-cell failure and diabetes in mice with a deletion mutation of the endoplasmic reticulum molecular chaperone gene P58IPK. Diabetes *54*, 1074–1081.

Lee, T.G., Tang, N., Thompson, S., Miller, J., and Katze, M.G. (1994). The 58,000-dalton cellular inhibitor of the interferon-induced double-stranded RNA-activated protein kinase (PKR) is a member of the tetratricopeptide repeat family of proteins. Mol. Cell. Biol. *14*, 2331–2342.

Lee, A.H., Iwakoshi, N.N., and Glimcher, L.H. (2003). XBP-1 regulates a subset of endoplasmic reticulum resident chaperone genes in the unfolded protein response. Mol. Cell. Biol. *23*, 7448–7459.

Matlack, K.E., Misselwitz, B., Plath, K., and Rapoport, T.A. (1999). BiP acts as a molecular ratchet during posttranslational transport of prepro-alpha factor across the ER membrane. Cell *97*, 553–564.

Melville, M.W., Tan, S.L., Wambach, M., Song, J., Morimoto, R.I., and Katze, M.G. (1999). The cellular inhibitor of the PKR protein kinase, P58(IPK), is an influenza virus-activated co-chaperone that modulates heat shock protein 70 activity. J. Biol. Chem. *274*, 3797–3803.

Meusser, B., Hirsch, C., Jarosch, E., and Sommer, T. (2005). ERAD: The long road to destruction. Nat. Cell Biol. *7*, 766–772.

Misselwitz, B., Staeck, O., and Rapoport, T.A. (1998). J proteins catalytically activate Hsp70 molecules to trap a wide range of peptide sequences. Mol. Cell *2*, 593–603.

Mitchell, D.M., Zhou, M., Pariyarath, R., Wang, H., Aitchison, J.D., Ginsberg, H.N., and Fisher, E.A. (1998). Apoprotein B100 has a prolonged interaction with the translocon during which its lipidation and translocation change from dependence on the microsomal triglyceride transfer protein to independence. Proc. Natl. Acad. Sci. USA *95*, 14733–14738.

Oyadomari, S., Koizumi, A., Takeda, K., Gotoh, T., Akira, S., Araki, E., and Mori, M. (2002). Targeted disruption of the Chop gene delays endoplasmic reticulum stress-mediated diabetes. J. Clin. Invest. *109*, 525–532.

Pariyarath, R., Wang, H., Aitchison, J.D., Ginsberg, H.N., Welch, W.J., Johnson, A.E., and Fisher, E.A. (2001). Co-translational interactions of apoprotein B with the ribosome and translocon during lipoprotein assembly or targeting to the proteasome. J. Biol. Chem. *276*, 541–550.

Patil, C., and Walter, P. (2001). Intracellular signaling from the endoplasmic reticulum to the nucleus: The unfolded protein response in yeast and mammals. Curr. Opin. Cell Biol. *13*, 349–355.

Scheufler, C., Brinker, A., Bourenkov, G., Pegoraro, S., Moroder, L., Bartunik, H., Hartl, F.U., and Moarefi, I. (2000). Structure of TPR domain-peptide complexes: Critical elements in the assembly of the Hsp70-Hsp90 multichaperone machine. Cell *101*, 199–210.

Shen, X., Ellis, R.E., Lee, K., Liu, C.-Y., Yang, K., Solomon, A., Yoshida, H., Morimoto, R., Kurnit, D.M., Mori, K., and Kaufman, R.J. (2001). Complementary signaling pathways regulate the unfolded protein response and are required for *C. elegans* development. Cell *107*, 893–903.

Sitia, R., and Braakman, I. (2003). Quality control in the endoplasmic reticulum protein factory. Nature *426*, 891–894.

Tsai, B., Ye, Y., and Rapoport, T.A. (2002). Retro-translocation of proteins from the endoplasmic reticulum into the cytosol. Nat. Rev. Mol. Cell Biol. *3*, 246–255.

Van Huizen, R., Martindale, J.L., Gorospe, M., and Holbrook, N.J. (2003). P58IPK, a novel endoplasmic reticulum stress-inducible protein and potential negative regulator of eIF2α signaling. J. Biol. Chem. *278*, 15558–15564.

Vogel, J.P., Misra, L.M., and Rose, M.D. (1990). Loss of BiP/GRP78 function blocks translocation of secretory proteins in yeast. J. Cell Biol. *110*, 1885–1895.

Yan, W., Frank, C.L., Korth, M.J., Sopher, B.L., Novoa, I., Ron, D., and Katze, M.G. (2002). Control of PERK eIF2-α kinase activity by the endoplasmic reticulum stress-induced molecular chaperone P58IPK. Proc. Natl. Acad. Sci. USA *99*, 15920–15925.

Ye, Y., Meyer, H.H., and Rapoport, T.A. (2001). The AAA ATPase Cdc48/p97 and its partners transport proteins from the ER into the cytosol. Nature *414*, 652–656.

Yu, H., Kaung, G., Kobayashi, S., and Kopito, R.R. (1997). Cytosolic degradation of T-cell receptor alpha chains by the proteasome. J. Biol. Chem. *272*, 20800–20804.

Zhang, J.X., Braakman, I., Matlack, K.E., and Helenius, A. (1997). Quality control in the secretory pathway: The role of calreticulin, calnexin and BiP in the retention of glycoproteins with C-terminal truncations. Mol. Biol. Cell *8*, 1943–1954.